EVALUATION OF SPACEBORNE AND AIRBORNE LINE SCANNER IMAGES USING A GENERIC ORTHO IMAGE PROCESSOR

Rupert Müller, Manfred Lehner, Peter Reinartz, Manfred Schroeder

DLR (German Aerospace Center), Remote Sensing Technology Institute, 82234 Wessling, Germany
Rupert.Mueller@dlr.de

Commission I, WG I/5

KEY WORDS: ortho image, direct georeferencing, airborne and spaceborne line scanner

ABSTRACT:
One of the main processing steps of evaluating remote sensing data is the production of ortho images from the acquired raw scanner data. Since in most applications of thematic analysis, a rectified data set is required, there is a need for an effective – regarding time and accuracy - and generic – regarding different sensor systems – processor for performing this rectification for any desired sensor imagery. This is especially true when using the image data in Geographic Information Systems (GIS) and for data fusion and analysis with data from different sources or seasons. The accuracy of this rectification result is crucial for overlaying the data with existing data sets or maps and using them for evaluations like change detection, map updating a.o.. Triggered by the demand of an automatic processor embedded in the Data Information and Management System DIMS of DLR a generic ortho image tool was developed.
The generic ortho image processor supports the production of ortho images from airborne and spaceborne digital line scanner images, as well as images from frame cameras. It is based on the Direct Georeferencing model using measurements of the exterior orientation of the sensor platform or sensor itself, the interior orientation (sensor parameters) and a digital elevation model. For the interior orientation models for pushbroom, whiskbroom and frame cameras as well as sensor calibration tables are supported. For the exterior orientation local level co-ordinate frames (navigation frame, orbital frame), earth centred earth fixed (ECEF) co-ordinate frames and generic mapping frames are supported. An approximate processing in a map projection is provided for airborne scanner data. The boresight misalignment matrix and the lever arm values are part of the functional model. Map projections are included in the processor. It also includes a link to the atmospheric correction processor ATCOR, which is also part of the automatic processing chain within DIMS.
The ortho image processor is applied for different sensors like the spaceborne line scanners SPOT5 and Quickbird, and the airborne line scanners HyMap, ROSIS, DAIS and Daedalus. For the calibration of the boresight misalignment angles or attitude offset angles ground control information is used. The accuracy of the ortho images with and without ground control information is shown. For SPOT5 images with an absolute location accuracy of 1 to 2 pixels using only the metadata delivered by the image provider, few ground control points (about 2-4) are sufficient to reach horizontal accuracy in the sub-pixel range. For Quickbird a comparison example between ortho images produced with RPC (Rational Polynomial Coefficients) and DG (Direct Georeferencing) is shown. A series of ground control points at the airport base DLR Oberpfaffenhofen and surrounding area serves as geometric calibration field for the determination of the boresight misalignment angles of the airborne scanners, which are used within different flight campaigns. The achieved accuracy for the geometric calibrated airborne systems is demonstrated.

1. INTRODUCTION

Triggered by the demand of an automatic processing chain for evaluation of scanner data up to level L2 (radiometric, atmospheric and geometric correction) a generic ortho image processor was developed based on the rigorous model of direct georeferencing (DG). High-precision integrated GPS/IMU systems for airborne sensors or position determination in sub-meter range in combination with attitude measurements using startrackers and gyros for spaceborne sensors provoke DG increasingly to become state-of-the-art technique to produce ortho images. Nevertheless improvements by ground control information are furthermore tasks to retrieve physical parameters considering very precise position determination leaving attitude restitution the major task. A generic processor must include the manifold coordinate transformations to handle input data and to produce ortho images in any projection. Different definitions for the attitude reference system, as well as description of sensor models must be part of a generic processor.

2. DIRECT GEOREFERENCING

The basis for all direct georeferencing formulas is the collinearity concept, where the coordinates of an object point $\mathbf{r}^m$ expressed in any earth bound mapping coordinate frame are related to image coordinates $\mathbf{r}^s$ derived from the measured pixel position in the sensor's coordinate frame. The rigorous relationship between 2D image coordinates and 3D object coordinates is given by

$$\mathbf{r}^m = \mathbf{r}_s^m + s \cdot \mathbf{R}_b^m \cdot \mathbf{R}_s^b \cdot \mathbf{r}^s , \qquad (1)$$

where $\mathbf{R}_s^b$ denotes the rotation around the angles $\boldsymbol{\varepsilon} = (\varepsilon_1, \varepsilon_2, \varepsilon_3)$ from the sensor to the body coordinate frame, which has to be calibrated, and $\mathbf{R}_b^m$ denotes the rotation

around the angles $\boldsymbol{\psi} = (\omega, \varphi, \kappa)$ from the body to a mapping coordinate frame, which is derived from the angular measurements. The position of the sensor projection centre

$$\mathbf{r}_s^m = \mathbf{r}_p^m - \mathbf{R}_b^m \mathbf{r}_p^b + \mathbf{R}_b^m \mathbf{r}_s^b \quad (2)$$

is calculated from the measured position $\mathbf{r}_p^m$ reduced by the pre-mission measured lever arms $\mathbf{r}_p^b$ from the body frame origin to the measured position and $\mathbf{r}_s^b$ from the body frame origin to the sensor projection centre, both expressed in the body coordinate frame. For single imagery the scale factor *s* is determined by the intersection of the sensor pointing direction with a given DEM also expressed in the mapping coordinate frame. It is noted that the DEM transformation into the mapping frame should at least include a resampling to the image resolution or better.

The interior orientation is described by mapping column(i)/row(j) values to the sensor coordinate frame with the focal length *c* by

$$\mathbb{N} \rightarrow \mathbb{R}^3 : i \rightarrow \mathbf{r}^s = (x_i^s, y_i^s, -c)^T \text{ for line scanners} \quad (3)$$

$$\mathbb{N}^2 \rightarrow \mathbb{R}^3 : i, j \rightarrow \mathbf{r}^s = (x_{i,j}^s, y_{i,j}^s, -c)^T \text{ for frame cameras.}$$

After object point reconstruction within the mapping frame it is transformed to any desired map projection, where the resampling of the ortho image proceeds.

As mentioned before the boresight alignment matrix $\mathbf{R}_s^b$ has to be determined using a calibration field with well measured ground control points (GCP). Assuming the exterior orientation is well measured the relation between image space and object space is after rearranging equation 1 of form

$$x^s = f_x(\mathbf{r}^m; \boldsymbol{\varepsilon}) \quad (4)$$

$$y^s = f_y(\mathbf{r}^m; \boldsymbol{\varepsilon}),$$

where the functions $f_{x/y}$ depend also on the three unknown boresight alignment angles. Introducing the image coordinates x_{GCP}^s, y_{GCP}^s (measured in sub-pixel range) and the object space coordinates $\mathbf{r}_{GCP}^m$ (well identifiable points w.r.t. the image resolution) of the GCP into the linearized equation 4 leads to

$$x_{GCP}^s - x^s\Big|_{GCP} = \sum_i \frac{\partial f_x}{\partial \varepsilon_i}\Big|_{GCP} d\varepsilon_i \quad (5)$$

$$y_{GCP}^s - y^s\Big|_{GCP} = \sum_i \frac{\partial f_y}{\partial \varepsilon_i}\Big|_{GCP} d\varepsilon_i ,$$

where the functions $f_{x/y}$ are evaluated at the GCP using interpolated values of the exterior orientation.

For a set of GCPs (min. 2) the system of linear equations is solved by iterative least squares adjustment. The same procedure can be applied to determine offsets of the measured orientation angles or positions. Simultaneous estimation of parameter sets (including interior orientation parameters) from single imagery has to be handled carefully due to the correlation of the parameters. The accuracy of the measurements, especially of the ephemeris data of spaceborne sensor systems or the exterior orientation of airborne sensor systems by high-end integrated GPS/IMU, yields hope to estimate physical orientation parameters from single imagery.

3. PROCESSOR FEATURES

From this principle point of view of DG a generic approach can be established suited for different sensor systems (see also: Müller, 2002). The major features in comprehensive form are:

Definitions of coordinate frames:
The model or mapping frame *m* is a local topocentric system (LTS/datum WGS84) with a fundamental point near the centre of the ortho image, with directions x to east, y to north and z perpendicular up to the WGS84 ellipsoid surface. The sensor coordinate frame has its origin at the camera projection center with (roughly spoken) x along track positive to motion direction, z up and y completes right handed triad. Additionally map projections like UTM can serve as mapping frame for airborne imagery.

Transformations of coordinate frames:
In order to transform ephemeris or DEM data to the mapping frame or to produce ortho images in any map projection a collection of 32 coordinate transformations with about 110 predefined as well as free geodetic datum transformations are part of the processor. The undulation w.r.t. WGS84 is taken from the EGM96 (Earth Gravity Model) for conversion from geoid to ellipsoid heights.

Interior orientation:
The interior orientation is described by models for whiskbroom, pushbroom and frame cameras or tables of 3D vectors for each sensor pixel according to equation 3, derived from laboratory or in –flight calibration.

Attitude angles:
The attitude angles can be measured with respect to the local level aircraft navigation frame, ECEF (Earth Centred Earth Fixed) or satellite orbit coordinate frame, where any sequence and direction of rotation is supported. The modelling of the attitude angles are explained in the following chapters. Angles represented in unit quaternion are transformed to Euler angles.

Positions:
The functional model includes the calculation of the position of the sensor projection centre using measured lever arm values. For airborne sensors using integrated GPS/IMU systems the position of the sensor projection centre is normally provided by separate navigation processing software from the manufacturers and for satellite sensors the lever arms are often neglected or already taken into account.

Resampling:
Bilinear or nearest neighbour resampling in irregular grids are supported.

Special functions:
Correction of systematic errors in angular rates during roll movements of optomechanical scanners can be taken into account.

For image matching demands in evaluation of stereo data quasi-epipolar images with information on reconstruction of image space coordinates can be produced.

A link to the atmospheric correction processor ATCOR, realized by sun-target-sensor geometry data for each pixel of the ortho image is included.

Restrictions:
The application of an automatic ortho image processor is restricted by coding special, mostly simple pre-processing software for each sensor system to transcribe the metadata into the ortho processor compatible format or to synchronise and interpolate the exterior orientation with imaging elements.

4. APPLICATIONS

The ortho image processor was applied to different spaceborne and airborne line scanner images. The accuracies of the ortho images were checked using ground control information and image matching techniques for co-registration assessment.

4.1 SPOT 5

Data material:
The area is located in Catalonia (Spain) and includes the city of Barcelona, covering dense urban areas as well as mountainous terrain. The data of Catalonia have been acquired on October 15th 2002 with a sun elevation of 39º and no clouds.

- Two sets of 8 bit panchromatic HRS stereo image data (size 12000 x 12000 pixel = 120 km across x 60 km along track) of Catalonian test area from two viewing directions of about ±20° stereo angle and 10m ground resolution, but along track sampling pitch of 5m.
- An 8 bit HGR panchromatic nadir looking HMA image with a ground resolution of 5 m x 5 m of part of the test site (size 12000 x 12000 pixel = 60 km across x 60 km along track)
- XML-files containing all additional information regarding time synchronization, position (DORIS), attitude (ULS: star tracking unit to compute absolute orientation in a celestial frame combined with the attitude orbit control system AOCS), interior orientation (tabulated look angles for each pixel)

Additional data are the following:

- colour ortho images (1:5000) with pixel size of 0.5 meter and accuracy better than 1 pixel (1σ)
- DEM with pixel spacing 15.0 meter and orthometric height accuracy of 1.1 meter (1σ)

Both reference data sets (ortho images and DEM) are provided in UTM zone 31 with the geodetic datum ED50 (European Datum 1950).

Modelling:
In a pre-processing step Lagrange interpolation of the ephemeris data (satellite position and velocity w.r.t. ITRF90 datum) and linear interpolation of the attitude angles (Euler angles w.r.t. orbit coordinate frame) serves for synchronisation with the image lines using scene centre time and sampling period. The attitude observations for each scan line at time *t* are modelled as follows

$$\mathbf{R}_b^m(t) = \mathbf{R}_{ECEF}^{LTS} \cdot \mathbf{R}_{orbit}^{ECEF}(t) \cdot \mathbf{R}_{body'}^{orbit}(t) \cdot \mathbf{T}_{body}^{body'} \qquad (6)$$

where the axes sorting matrix $\mathbf{T}_{body}^{body'}$ describes a rotation of -90° around the z-axis to permute across and negative along track sensor coordinates, the matrix

$$\mathbf{R}_{body'}^{orbit} = \mathbf{R}_x(\alpha_1) \cdot \mathbf{R}_y(\alpha_2) \cdot \mathbf{R}_z(-\alpha_3) \qquad (7)$$

build by the measured Euler angles $\boldsymbol{\alpha} = (\alpha_1, \alpha_2, \alpha_3)$ and the direction cosine matrix build by the unit orthogonal basis vectors, spanning the orbit frame

$$\mathbf{R}_{orbit}^{ECEF} = \left(\frac{(\mathbf{r}\times\mathbf{v})\times\mathbf{r}}{\|(\mathbf{r}\times\mathbf{v})\times\mathbf{r}\|}, \frac{\mathbf{r}\times\mathbf{v}}{\|\mathbf{r}\times\mathbf{v}\|}, \frac{\mathbf{r}}{\|\mathbf{r}\|} \right) \qquad (8)$$

with **r** the interpolated satellite position and **v** the interpolated satellite velocity expressed in ECEF coordinate frame (ITRF90 and WGS84 assumed identical).
The interior orientation, determined by pre- and in-flight calibration, is tabulated for each pixel containing already the stereo angles for the HRS sensors. (SPOT IMAGE, 2002)

Results:
It was shown that even without any ground control, the absolute georeferencing accuracy of the HRS sensor is in the order of one to two pixel, less than 20 meter and standard deviation less than one 1 pixel (Reinartz, 2004). This is in line with the predicted absolute pointing accuracy of about 33 meters with 90% accuracy. By automatic matching of the HRS ortho images a very homogeneous behavior of the difference vectors was found, which suggests an improvement of the pointing accuracy by few GCPs. The satellite position determination with the DORIS system is in sub-meter range and variations of georeferencing accuracy is linked to changes w.r.t. solar exposure during orbit revolution (latitudinal model) (Bouillon, 2003), which advises corrections of the relative orientation of the instruments. Selecting different sets of GCPs for estimation of boresight alignment angles a series of ortho images from the forward and backward looking sensors are generated and compared by image matching. The distribution of the GCPs is shown in figure 1.

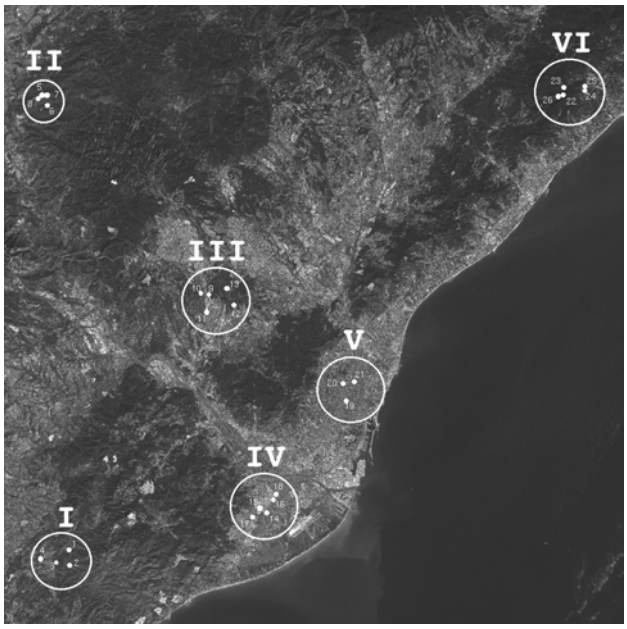

Figure 1: Distribution of GCP groups at Catalonia test site selected from reference ortho images. Flight direction is from top to bottom.

The co-registration deviation (table 1) decreases from 1.3 pixels (=13m) RMSE north/south with no ground control information to 0.3 pixels (=3m) RMSE north/south using all 28 GCPs. For the two evaluations with 3 GCPs (I/V/VI and I/IV/VI) the best three-way combination (I/IV/VI) and a worse combination (I/V/VI) in the sense of RMSE at the GCPs after improvement was chosen. The same was done for two four-way GCP combinations (2 x I/IV/V/VI). In both cases the best GCP

combinations reach the same co-registration accuracy as the usage of all GCPs. This implies that with 3 to 4 well measured GCPs the same accuracy can be reached provided they are distributed over the swath (see figure 1). It is an interesting fact, that the RMSE values for each HRS1 and HRS2 at the GCPs after improvement is of magnitude 0.5 pixels (input data: all GCPs), whereas after modeling the residuals obtained by matching drop to 0.3 pixels.

Table 1: Matching results between ortho images from HRS1 and HRS2 before and after improvement, and with different combinations of GCPs (1 pixel = 10m)

HRS1 versus HRS2	Matching Points [#]	RMSE North [pixel]	RMSE East [pixel]	RMSE north/south [pixel]
no GCP	88897	0.49	1.23	1.32
I/VI	94570	0.94	0.23	0.97
I/V/VI	98671	0.59	0.18	0.62
I/IV/VI	103311	0.33	0.15	0.36
I/IV/V/VI	104019	0.42	0.20	0.47
I/IV/V/VI	99956	0.19	0.18	0.27
28 GCPs	111039	0.26	0.15	0.30

Additionally the co-registration accuracy of the stereo channels HRS1 and HRS2 with the nadir looking channel HMA were investigated. Here the matching differences, in comparison to HRS1-HRS2, of the uncorrected ortho images (arrows in Fig. 2) show variable shift, which depends on the position in the CCD array (Müller, 2004).

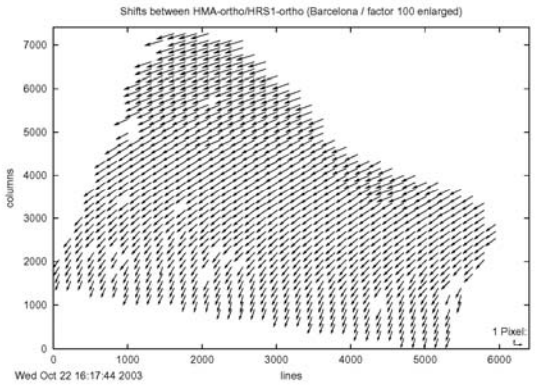

Figure 2: Shifts between the two ortho images derived from forward and nadir looking channels of SPOT HRS and HMA (mean values in a regular grid)

After estimation of the orientation angles of HMA with 29 GCPs the co-registration accuracy reaches RMSE of 4-5m less than between the stereo channels (table 2).

Table 2: Matching results between ortho images HRS1-HMA and HRS2-HMA with all GCPs (1 pixel = 10m)

	Matching Points [#]	RMSE North [pixle]	RMSE East [pixel]	RMSE north/south [pixel]
HMA-HRS1	18263	0.24	0.42	0.49
HMA-HRS2	23898	0.31	0.24	0.39

4.2 Quickbird

Data material:

A multispectral Quickbird (QB) image of product level 1B stereo from Esfahan (Iran) with a ground resolution of 2.4m, 1.4° cross-track angle and 29° off-nadir view angle was available, together with the metadata including attitude, ephemeris and geometric calibration data. A DSM of SRTM C-Band was used for ortho image generation by DG. An ortho image derived from RPF (Rational Polynomial Functions) served as comparison image (Lehner, 2005).

Modelling:

The ephemeris data, measured w.r.t. the ECEF (datum WGS84) are interpolated (Lagrange interpolation) for each scan line using the time of the first line and the sampling rate. The attitude data are given in unit quaternions, which were transformed to orthogonal matrix representation and from there Euler angles of sequence roll-pitch-yaw were extracted. By linear interpolation the attitude angles for each scan line from the body to ECEF coordinate frame is generated (note: interpolation in quaternion space must be carried out on the unit hypersphere).

$$\mathbf{R}_b^m(t) = \mathbf{R}_{ECEF}^{LTS} \cdot \mathbf{R}_{body}^{ECEF}(t) \tag{9}$$

The rotation from the camera coordinate frame to the body frame, expressed in unit quaternion, is derived from the given metadata (transformation to Euler angles), where $\mathbf{T}$ is a rotation of 180° around the x-axis accounting for the spacecraft coordinate frame definition from QB.

$$\mathbf{R}_s^b = \mathbf{R}_{sensor'}^{body} \cdot \mathbf{T}_{sensor}^{sensor'} \tag{10}$$

The interior orientation is derived from origin X/Y values of the first pixel of the CCD array, the sampling pitch and the focal length values of the metadata (Level 1B images are already corrected for lens distortions and CCD rotations). (DIGITALGLOBE, 2004)

Results:

Because no ground control information from test site Esfahan is available an absolute accuracy assessment of the ortho images is not possible. Therefore a comparison of ortho images generated with RPF and DG is shown. The matching results between these images are shown in table 3.

Table 3: Quickbird matching result between ortho images produced with RPC and DG (1pixel = 2.4m)

matching points	Mean north	Mean east	STDV north	STDV east
205744	6.26	-1.18	0.42	0.11

The high deviation in mean north direction of about 15m can not be explained yet. As shown in figure 3 a high STDV occurred in the middle part, where mountainous area dominates. An error in the DSM will have an large effect on the 29° forward looking channel (flight direction is roughly from left to right in figure 3).

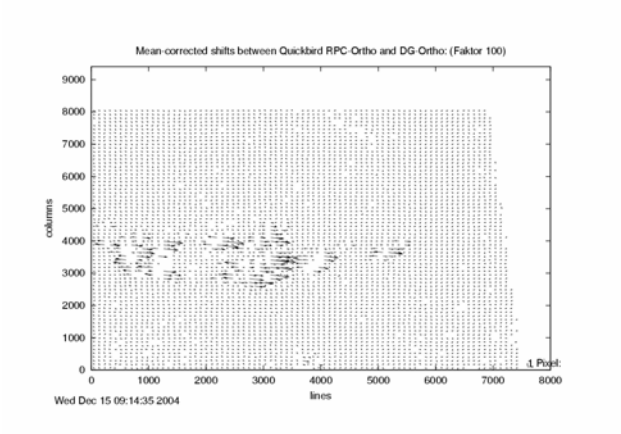

Figure 3: Mean corrected shifts between the two ortho images generated with RPF and DG method (mean values in a regular grid)

4.3 Airborne Sensors

For airborne sensor systems high-precision IMU/GPS provide exterior orientation elements for DG. The boresight alignment angles have to be calibrated after each installation in the aircraft. The IMU has to be rigidly mounted on the sensor to avoid independent movements of the sensor and the IMU.

Data material:
For the accuracy assessment ortho images of four different multi- and hyperspectral sensors (see table 4) were investigated. The image data were aquired from the same test site located at DLR Oberpfaffenhofen.

Table 4: Investigated airborne sensors and mission parameters

Sensor	ROSIS	DAIS	Daedalus	HyMap
Sensor type P: pushbroom W: whiskbroom	P	W	W	W
FOV [°]	17.37	51.20	85.92	61.3
IFOV [mrad]	0.59	3.3	2.5	2.09
altitude above ground [m]	3230	3230	2030	2370
footprint [m]	1.9	10.7	5.1	4.9

For the flight mission with the sensors ROSIS-03, DAIS-7915 and Daeadalus-ATM-1256 the IGI CCNS/AEROcontrol-IIb and for HyMap the Cmigit position and orientation system (NAV) was used. The performances (RMSE) given by the manufacturers is listed in table 5. It is noted, that the proceeding system of IGI with fibre-optic gyros (IMU-IId) reaches attitude accuracies of 0.005° RMSE (Grimm, 2001).

Table 5: Performance of the NAV systems given by the manufacturers.

	AEROcontrol IIb	Cmigit
Position[m]	0.1–0.3 DGPS mode 1-3 OmniStar	2.5 horizontal 3.0 vertical
roll&pitch[°]	0.01	0.06
Heading[°]	0.1	0.09

Simulations (see table 6) using the performance specifications and the mission parameters show the expected accuracy (RMSE) for nadir view / max scan angle of the different sensor/NAV systems at the corresponding flight altitude (for Daedalus the OmniStar service was used).

Table 6: Expected accuracy w.r.t. NAV system

	ROSIS	DAIS	Daedalus	HyMap
DX[m]	0.6 / 1.0	0.6 / 2.8	2.0 / 3.9	3.5 / 4.2
DY[m]	0.6 / 0.6	0.6 / 0.7	2.0 / 2.1	3.5 / 4.2
DXY[m]	0.9 / 1.2	0.9 / 2.9	2.9 / 4.4	5.0 / 5.9

A DEM derived from the ERS-1/2 Tandem mission with 5-10m vertical accuracy and 25m horizontal resolution served as input for the rectification of the three images. The comparison of this DEM with a DEM (covering only partially the test site) derived from a aerial image stereo pair emphasises the accuracy of the used DEM with mean height differences less than one meter measured at six corresponding points.

Modelling:
The attitude observations for each scanline at time t are modelled as follows

$$\mathbf{R}_b^m(t) = \mathbf{R}_{ECEF}^{LTS} \cdot \mathbf{R}_{NAV'}^{ECEF}(t) \cdot \mathbf{T}_{NAV}^{NAV'} \cdot \mathbf{R}_{IMU}^{NAV}(t) \tag{11}$$

where the roll, pitch and heading angles are measured from the GPS/IMU system w.r.t. the local level coordinate frame. By definition only the z- component could have non-zero values in this case (therefore also the local orthogonal longitude/latitude system can be used). Due to the different definition of the body coordinate frame in ARINC 705 norm it is obtained

$$\mathbf{R}_{IMU}^{NAV} = \mathbf{R}_z(heading) \cdot \mathbf{R}_y(pitch) \cdot \mathbf{R}_x(-roll) \tag{12}$$

The axes-sorting matrix $\mathbf{T}_{NAV}^{NAV'}$ describes the change from north-west-up to east-north-up coordinate frame. The position of the sensor projection centre is already provided by an independent processing.

Results:
For all four airborne sensors the boresight alignment angles (rotation sequence: first X-Y-Z last) are estimated using few (DAIS/Daedalus) and more (HyMap/Rosis) GCPs. The high angle of about 4° for Rosis is explained by the tilted mirror in backward direction (table 7).

Table 7: RMSE at GCPs for the airborne sensors before and after borsight alignment angle calibration in order along/across

Sensor	HyMap	Daedalus	DAIS	Rosis
GCP [#]	22	5	7	25
RMSE at GCP	5.50	1.44	7.80	122.99
before [pixel]	1.60	3.13	4.45	11.34
RMSE at GCP	0.40	0.35	0.62	1.01
after [pixel]	0.51	0.99	0.67	1.05
Boresight	-0.046	-0.347	-0.424	0.366
Angles [°]	-0.602	0.165	0.770	-4.205
	0.216	0.058	-0.279	-0.001

With the estimated boresight alignment angles ortho images, resampled to a pixel size of 5x5m², are generated and the accuracy of co-registration of ortho image pairs investigated by image matching (table 8). Due to the different spectral ranges and acquisition dates only few good matching points are found.

Table 8: Matching results of pairs of ortho images (1 pixel = 5m)

Combination	DAIS – Daedalus	Daedalus – HyMap	Rosis – Daedalus
Matching Points [#]	63	92	126
Mean [pixel] line/column	0.51 -0.41	-0.19 0.50	-0.12 -0.50
STDV [pixel] line/column	0.25 0.51	0.22 0.50	0.12 0.25
Minimum [pixel] line/column	0.32 -1.31	-0.52 -0.64	-0.36 -0.99
Maximum [pixel] line/column	1.09 0.39	0.30 1.56	-0.08 -0.34

For all matching combinations of the individually corrected ortho images a co-registration in each direction of <0.51 pixel (<2.6m) with a deviation of less than half a pixel size (=2.5m) is found, which is in line with the expected accuracy (table 6). It is noted, that for the interior orientation ideal sensor models are used (also for the CCD camera ROSIS) and the accuracy of the DEM influences the accuracy of the ortho image especially for sensors having a wide FOV. The direct comparison of the Daedalus ortho image with manually measured (sub-pixel range) control points emphasis the matching result with better mean deviations of < 0.3 pixel (<1.4 m) and about the same standard deviation of about 0.5 pixel (table 9).

Table 9: Accuracy assessment of Daedalus ortho image using 41 ground control points

Direction	East	north
Mean [pixel / m]	0.27 / 1.37	-0.16 / -0.81
STDV [pixel / m]	0.53 / 2.68	0.38 / 1.89

5. CONCLUSION

The generation of ortho images based on direct georeferencing is applied to space- and airborne scanner data. The main results are:

- For SPOT5 HRS1-HRS2 images a co-registration accuracy of 3m (=0.3 pixel) RMSE can be reached using 3-4 good GCPs used for improvement of the relative orientations of the instruments. SPOT5 HMA-HRS co-registration accuracy reaches RMSE values of 4-5m.
- For Quickbird Level 1B MUL image a comparison between DG and RPF generated ortho images show a mean deviation of about 15m in flight direction, which is also the off-nadir view direction of 29° and 2m across track direction. An explanation cannot be given yet.
- The estimation of the boresight alignment angles for four airborne sensors leads to absolute co-registration accuracies of <2.6m with standard deviations of about 2.5m for each planar direction. This is in line with the predicted accuracy of the used GPS/IMU systems of medium performance. State-of-the-art systems, with much better attitude determination will increase the accuracies.

An ortho image processor based on DG was presented, which comprises features to handle a lot of different sensor/NAV systems.

ACKNOWLEDGEMENT

The authors like to thank Monika Harbich and Manuela Poetzsch for the manual measurements and supporting the investigations.

REFERENCES

Bouillon, A. ; Breton, E. ; De Lussy, F. ; Gachet, R.
"SPOT5 Geometric Image Quality", *IGARSS 2003, Toulouse, 21.-25. July 2003, IEEE International Geoscience and Remote Sensing Symposium*

DIGITALGLOBE,
"QuickBird Imagery Products", *Product Guide, Revision 4.3, Release date 2004*

Grimm, A., Results of the integrated CCNS AEROcontrol System, *OEEPE Workshop, Integrated Sensor Orientation*, *Hannover 2001*

Lehner, M., Müller, R., Reinartz, P.
„DSM and Orthoimages from Quickbird and IKONOS Data using Rational Polynomial Functions", *High-Resolution Earth Imaging for Geospatial Information, ISPRS Hannover Workshop 2005*

Müller, R., Lehner, M., Reinartz, P., Schroeder, M.; Vollmer,B.
„A Program for direct georeferencing of airborne and spaceborne line scanner images", *Proceedings of ISPRS Commission I Mid-Term Symposium "Integrating Remote Sensing at the Global, Regional and Local Scale", 2002, Denver CO, Vol. XXXIV, Part 1, Commission I*

Müller, R., Reinartz, P., Lehner, M., Schroeder, M.
"Comparison of the Accuracy of DEM from SPOT HRS two-fold Stereo Data and HRS/HRG three-fold Stereo Data in Barcelona Test Site", *Proceedings of the ISPRS XXth Congress, Istanbul 12-23 July 2004*

Reinartz, P., Lehner, M. Müller, R. Schroeder, M.,
"Accuracy for DEM and Orthoimages derived from SPOT HRS Stereo Data without using GCP", Proceedings of the ISPRS XXth Congress, Istanbul 12-23 July 2004

SPOT IMAGE,
"SPOT Satellite Geometry Handbook", *S-NT-73-12-SI, Edition 1, Rev. 0, Toulouse, France 2002*